Analyst

Carbohydrate Isomer Resolution via Multi-site Derivatization Cyclic Ion Mobility-Mass Spectrometry

Journal:	*Analyst*
Manuscript ID	AN-ART-08-2019-001584.R1
Article Type:	Paper
Date Submitted by the Author:	21-Oct-2019
Complete List of Authors:	McKenna, Kristin; Georgia Institute of Technology College of Sciences, School of Chemistry and Biochemistry Li, Li; Georgia Institute of Technology, Schools of Chemistry and Chemical Engineering; University of Texas Southwestern Medical Center at Dallas Baker, Andy; Waters Corp Ujma, Jakub; Waters Corp Wilmslow Krishnamurthy, Ramanarayanan; TSRI, Chemsitry Liotta, Charles; Georgia Institute of Technology, Schools of Chemistry and Chemical Engineering Fernandez, Facundo; Georgia Institute of Technology, School of Chemistry and Biochemistry

Analyst

ARTICLE

Received 00th January 20xx,
Accepted 00th January 20xx
DOI: 10.1039/x0xx00000x

www.rsc.org/

Carbohydrate Isomer Resolution *via* Multi-site Derivatization Cyclic Ion Mobility-Mass Spectrometry.

Kristin R. McKenna[ab], Li Li[abc], Andy Baker[d], Jakub Ujma[e], Ramanarayanan Krishnamurthy[af], Charles L.Liotta[ab] and Facundo M. Fernández[ab*]

Oligosaccharides serve many roles in extant life and may have had a significant role in prebiotic chemistry in early Earth. In both these contexts, the structural and isomeric diversity among carbohydrates presents analytical challenges necessitating improved separations. Here, we showcase a chemical derivatization approach, where 3-carboxy-5-nitrophenylboronic acid (3C5NBA) is used to label vicinal hydroxyl groups, amplifying the structural difference between isomers. We explore the applicability of state-of-the-art ion mobility – mass spectrometry (IM-MS) instrumentation in the analysis of derivatized carbohydrates. In particular we focus on the resolving power required for IM separation of derivatized isomers. A recently developed cyclic ion mobility (cIM) mass spectrometer (MS) was chosen for this study as it allows for multi-pass IM separations, with variable resolving power (R_p). Three passes around the cIM (R_p~120) enabled separation of all possible pairs of four monosaccharide standards, and all but two pairs of eight disaccharide standards. Combining cIM methodology with tandem mass spectrometry (MS/MS) experiments allowed for the major products of each of the 3C5NBA carbohydrate derivatization reactions to be resolved and unequivocally identified.

Introduction

Understanding the chemical processes leading to the origins of life on Earth is one of the greatest scientific questions of our time.[1] With the Miller-Urey experiment[2] leading to decades of scientific research in prebiotic chemistry, the non-enzymatic origin of biopolymers such as nucleic acids and peptides has been studied at length.[3-5] Carbohydrates are also critical components of life, and are responsible for maintaining cell structure, intercellular communication, and various other central biological processes.[6-10] As carbohydrates aid in the co-solubility of biopolymers, can serve as cross-linkers, and provide rudimentary catalytic activity, it is highly likely they were also important for the development of early life on the prebiotic Earth.[11]

The structures of mono- and oligosaccharides determine their properties and function, so it is critical that their characterization is performed beyond their molecular weight. For example, certain sugars are non-reducing and can protect other molecules from stress caused by pH or temperature changes, whereas reducing sugars can react with amino acids and other biologically-relevant molecules.[12-14] Carbohydrates are structurally diverse and complex, and have received less attention in prebiotic chemistry when compared to peptides and nucleic acids.[15-16] Polysaccharides contain a great diversity of monomeric units, each with several possible linkages, as well as the potential for branching. Additionally, each anomeric carbon can have either an α or β configuration, doubling the possible number of structures to be detected and resolved. Because of their identical elemental formulas, these isobars cannot be distinguished even with the use of ultrahigh resolution-mass spectrometry (MS).

Several analytical methods have been utilized to characterize oligosaccharides. Tandem mass spectrometry (MS/MS), for example, can efficiently distinguish relatively pure disaccharide samples. It cannot, however, effectively characterize lower abundance components in complex mixtures of isobaric carbohydrates.[17-18] Nuclear magnetic resonance (NMR) spectroscopy can also be very useful, but requires higher concentrations, and can therefore be more time consuming.[19-21] Liquid chromatography (LC) has been extensively used for disaccharide identification, but it is relatively slow and may require derivatization for higher resolution separations.[22-23] Capillary electrophoresis (CE) is also an effective method for carbohydrate separations, but some degree of *a priori* knowledge about the oligosaccharides being separated is typically required.[24-26]

Ion mobility (IM) separations coupled to mass spectrometric detection (IM-MS) have been shown to be a viable complement to other established, yet limited, techniques. This method requires lower sample concentrations than NMR, shorter analysis times than either NMR or LC and, with sufficient resolving power $\left(\boldsymbol{R_p} = \frac{t_d}{\Delta t_d}\right)$,[27] can distinguish isomeric species in complex mixtures. IM separations depend on the mobility coefficient (K), which determines the velocity of the gas phase

[a] NSF/NASA Center for Chemical Evolution
[b] School of Chemistry and Biochemistry, Georgia Institute of Technology, Atlanta GA 30332, USA.
[c] Current affiliation: Center for Alzheimer's and Neurodegenerative Diseases, Department of Biochemistry, University of Texas Southwestern Medical Center, Dallas, TX 75390, USA.
[d] Waters Corporation, Pleasanton, CA 94588, USA.
[e] Waters Corporation, Wilmslow SK9 4AX, United Kingdom.
[f] Department of Chemistry, The Scripps Research Institute, La Jolla, CA 92037, USA.
* E-mail: facundo.fernandez@chemistry.gatech.edu; Fax: +1 (404) 894-7452; Tel: +1 (404) 385-4432
Electronic Supplementary Information (ESI) available: [details of any supplementary information available should be included here]. See DOI: 10.1039/x0xx00000x

ions in the electric field. *K* depends on a variety of instrumental parameters, masses of ion and gas molecules, and their rotationally-averaged collision cross section (CCS). The latter parameter can be correlated to the 3D structure of ions.[28]

In this manuscript we focus on travelling wave IM spectrometry (TWIMS) where the mobility separator is comprised of a series of electrodes enclosed in a gas filled cell (~2 mbar N_2). A series of voltage pulses is applied sequentially to each electrode, propelling ions through the device.[29] Ions can "surf" or "roll over" the wave falling back into the preceding wave. Ions of lower mobility undergo more roll over events than higher mobility ions, effectively leading to mobility separation. Drift times (t_d) measured in TWIMS can be converted to CCS using calibration procedures.[30-32] A number of calibrant compounds have been proposed.[33] Resolving power (R_p) of an IM separator can be improved by increasing its length.[34] Recently, Giles *et al.* developed a travelling wave-enabled, cyclic IM (cIM) instrument with multi-pass capabilities.[35] In this instrument, IM resolving power increases as a function of the square root of the number of passes, *n* ($\boldsymbol{R_p \sim 70\sqrt{nz}}$);[35] here 70 is the approximate, single pass resolving power and z is the ion's charge state. Normally, the maximum number of passes is limited by the so called "wrap-around" effect that occurs when the spatial width of the separated ion packets exceeds the length of the cIM device.[36] The cIM control enables selective ejection of ions in a specified range of arrival times from the cIM device that can be followed by activation and/or further separation of product ions (IMS^n).[36-37] These functionalities have been used previously for structural studies of carbohydrate[37-38] and protein ions.[39]

Isomeric pentasaccharides, including anomers, have been shown to be able to be separated by the cIM system.[37] Typically, isobaric mono- and disaccharides do not have sufficiently-different CCS values to be separated by commercially-available IM systems. To mitigate this issue, shift reagents — ligands that can bind either covalently or non-covalently to amplify CCS differences between isobaric carbohydrates — have been utilized. Previous examples of shift reagents include alkali and alkaline earth metal cations, and 1-phenyl-3-methyl-5-pyrazolone.[40-42] In recent work, we reported a new shift reagent for carbohydrates, 3-carboxy-5-nitrophenyl boronic acid (3C5NBA) that rapidly reacts with mono- and disaccharides, enhancing their IM separation.[43] Due to the initial promise shown by 3C5NBA, we here evaluate its applicability in combination with high-resolution cIM-MS instrumentation. In addition, we utilized the tandem IMS (IMS^2) capability to probe the possibility of interconversion between mobility separated mannose derivatives.

Experimental

Reagents and Chemicals

Isomaltose, trehalose, cellobiose, D-fructose, and 3-carboxy-5-nitrophenylboronic acid (3C5NBA) were obtained from TCI (Philadelphia, PA). As stated by the manufacturer, the purchased 3C5NBA contained both the monomer and the anhydride dimer. This was verified by detection of the $[M-H]^-$ ions for these species at *m/z* 210.0 and 403.0, respectively, as shown in Figure S-1. Maltose, lactose, lactulose, sucrose, D-(+)-glucose, and D-(+) galactose were purchased from Sigma Aldrich (St. Louis, MO). Melibiose was obtained from Fluka. D-mannose was purchased from VWR.

Multi-site derivatization of carbohydrates

Stock solutions of carbohydrate standards (1 mM) were prepared in water. A 1 mM 3C5NBA stock solution was prepared in acetonitrile and kept refrigerated at 5 °C until used. Previously reported reaction methods were utilized.[43] In short, a solution of 5 µL of the 1 mM carbohydrate solution and 10 µL of the 1 mM 3C5NBA solution were incubated at room temperature for 5 minutes for disaccharides and 30 minutes for monosaccharides. The reaction mixture was then diluted to 1 mL with deionized water prior to IM-MS analysis.[44]

Ion mobility-mass spectrometry analysis

Ion mobility experiments were performed using either a standard SYNAPT G2-S*i* (Q-IM-ToF) or a prototype, quadrupole cyclic ion mobility orthogonal time-of-flight mass spectrometer (Q-cIM-ToF) (Waters, Wilmslow, UK).[45] All experiments used direct infusion electrospray ionization in negative ion mode. Instrument ion source settings were as follows: capillary voltage, 2.2 kV; cone voltage, 100 V; source offset, 60 V; source temperature, 100 °C; desolvation temperature, 250 °C; desolvation gas flow, 600 L h^{-1}; and cone gas flow, 50 L h^{-1}. For the SYNAPT G2-S*i*, the travelling wave height was 40 V, the travelling wave velocity was 500 m sec^{-1}, the helium cell was operated at 180 mL min^{-1}, and nitrogen was used as the IM gas (90 mL min^{-1}). For the cIM system, source parameters were the same as above; the helium cell was operated at 80 mL min^{-1} and nitrogen IM gas at 70 mL min^{-1}. The travelling wave height was 35 V and the travelling wave velocity was 375 m sec^{-1}. Mannose derivatives were investigated by IMS^2. Following three passes around the cIM, the separated ions were selectively ejected from the cIM device and re-injected using a higher voltage offset (115 V), resulting in activation. Activated ions were then subjected to additional three passes around the cIM device. This method was meant to probe whether certain features in the ATD could interconvert.

Arrival time distributions were extracted from MassLynx 4.2 into OriginPro 8.5 and fitted with Gaussian functions to more precisely determine peak maxima. Reported arrival times include the "dead time" (the time spent between the exit of the cIM and detector), which ranged from 6.29-6.78 ms for monosaccharide derivatives and 2.77-3.75 ms for disaccharide derivatives.

Tandem mass spectrometry (MS/MS) experiments

For MS/MS experiments, the ions of interest were quadrupole-selected and subjected to collision induced dissociation (CID) in the transfer region of the Q-cIM-ToF instrument following IM separation. The doubly derivatized monosaccharide precursor ions were selected at *m/z* 529.10, and the doubly derivatized disaccharide precursors were selected at *m/z* 691.13. The transfer collision energy was 18 eV for disaccharide derivatives, and 12 eV for monosaccharide derivatives.

Results and Discussion

Derivatization reactions

The four monosaccharide and eight disaccharide standards that were tested in this study are shown in Figure 1. Notably, maltose, trehalose, isomaltose, and cellobiose are all glucose dimers (*i.e.* glucopyranosyl-glucose isomers). Maltose and cellobiose are anomers, isomers that only differ in the stereochemistry of the anomeric carbon. The remaining disaccharides included in the study contained at least one of the monosaccharide units above. Glucose, galactose, and mannose are aldose epimers that differ only in their stereochemistry, while fructose is a ketose.

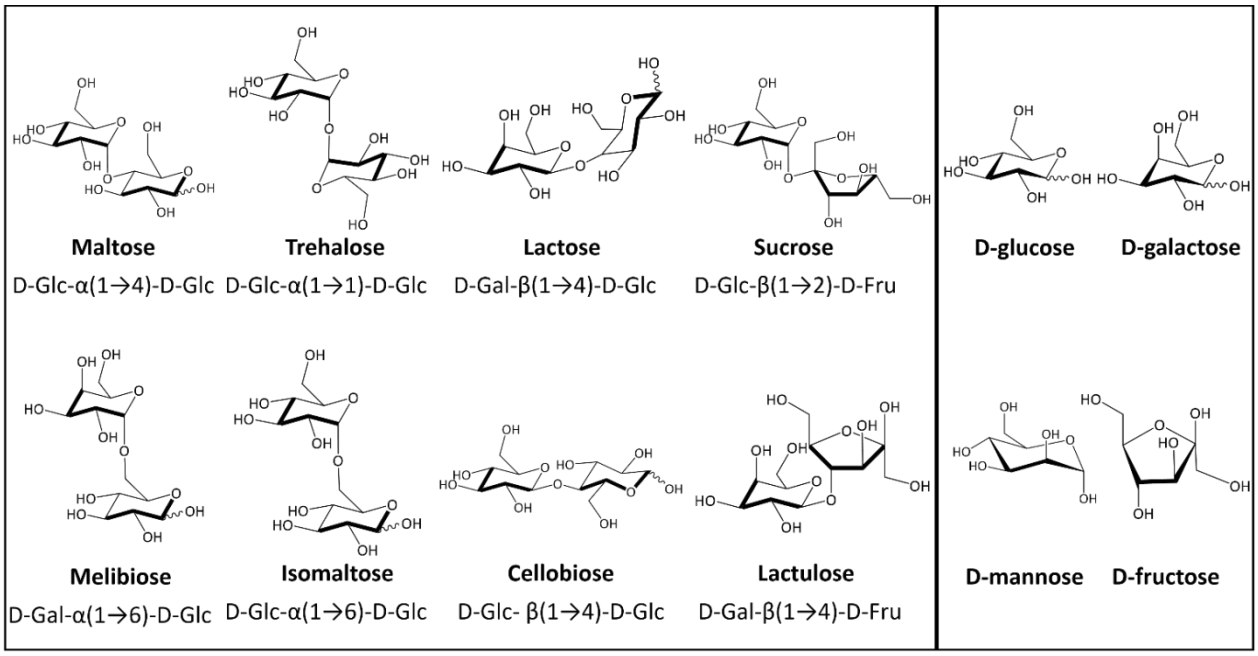

Figure 1. Structures of isobaric disaccharide and monosaccharide standards utilized in this study.

3C5NBA was selected as a shift reagent to amplify CCS differences between isomeric carbohydrates.[43] As an example, the 3C5NBA derivatization reaction for maltose is presented in Figure 2. Here, 3C5NBA can react with two different *cis* diols to form two rings with either five or six members as well as two *trans* diols on C_4 and C_6 to form a six-membered ring (Figure 2d).[46] Additionally, the 3C5NBA reagent also contains the anhydride dimer, as shown in Figure S-1. This anhydride, B-(3-carboxy-5-nitrophenylboronic acid)-3- carboxy-5-nitrophenylboronic acid, can react with two *trans* diols to form a seven-membered ring product (Figure 2a-c).[47] The number of expected products for each carbohydrate investigated as well as a breakdown of the products for each reagent (3C5NBA or its anhydride dimer) are shown in Table S-1. Although the fact that multiple products were formed by most of these reactions may somewhat limit the applicability of this derivatization reagent for quantitative experiments, the availability of multiple CCS values could also help confirm the analyte's identity when identifying unknowns. These doubly-derivatized products were chosen for further characterization by IM-MS.

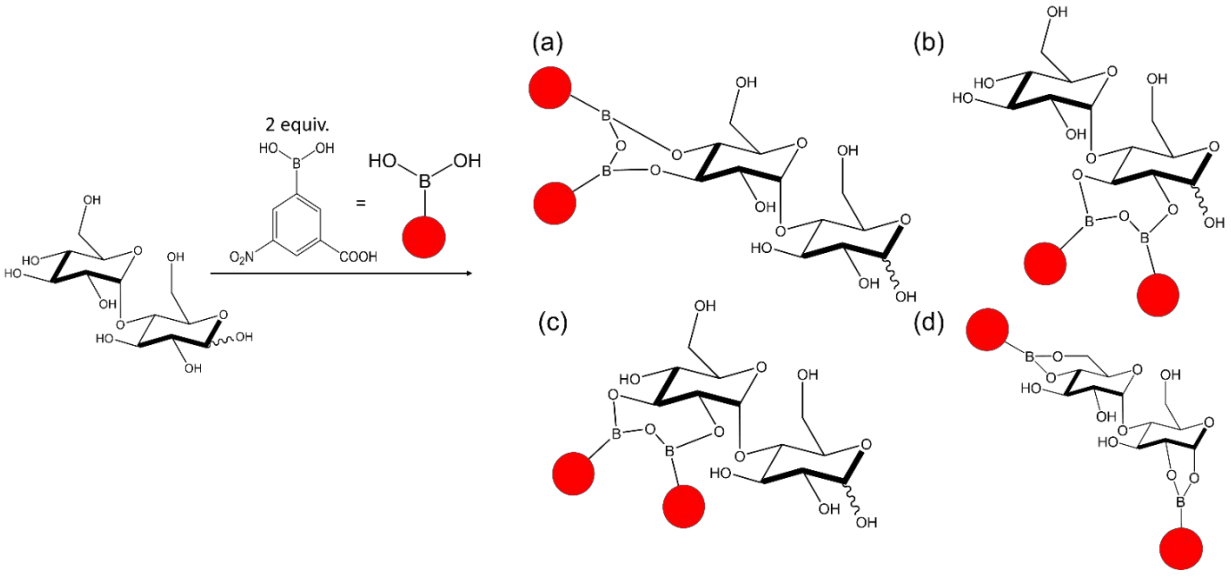

Figure 2. Example reaction scheme for maltose with 3C5NBA. The red circle indicates the 3-carboxy-5-nitrophenyl group in 3C5NBA. Anhydride derivatives were mainly observed as their water loss deprotonated ions $[M\text{-}H_2O\text{-}H]^-$.

Cyclic ion mobility analysis

Arrival time distributions (ATDs) of doubly-derivatized monosaccharides and disaccharides obtained after various passes around the cIM are shown in Figures 3 and 4, respectively. Each panel in the figure represents a single carbohydrate subjected to n=1, 2 and 3 passes around the cIM device. The corresponding, estimated R_p values were ~70, ~100 and ~120, respectively. As expected, the number of resolved features increased with n; these were attributed to positional and functional isomers with different 3C5NBA derivatization sites (Table S-1). For fructose, for example, two derivatives are expected, and two features appeared resolved in the ATD (Figure 3a). Similarly, three derivatives are expected for both galactose and glucose, and three features were seen in their ATDs (Figure 3b-c). In contrast, six derivatives are possible for sucrose, while only three features were resolved in the ATD (Figure 4g), likely due to spectral overlap or insufficient yield of some of the derivatives. Figure S-2 shows the peak areas for the glucose derivative observed after one, two and three passes around the cIM. In line with the previous observations by Giles *et al.*,[36] the transmission losses were minimal.

Although in most cases regio- and functional isomers of derivatized monosaccharides were resolved after one pass (Figure 3), this was not the case for derivatized disaccharides (Figure 4). For these analytes, the CCS shift introduced by 3C5NBA derivatization was proportionally smaller, and thus a higher number of passes around the cIM was required to resolve them. For example, only two isomers of doubly-derivatized cellobiose were resolved after one pass; however, after three passes five features were seen in the ATD (Figure 4a). Several other disaccharides were also observed to behave in a similar manner. For isomaltose, melibiose, sucrose, and trehalose, between two and three passes were sufficient to resolve two to three otherwise overlapping peaks. While further increasing the number of passes can be a powerful tool to improve R_p, there was a limit to the number of passes that could be performed without observing wraparound effects, as discussed by Giles *et al.*[36]

Some ATD features, such as those observed for mannose derivatives (Figure 3d), showed significant fronting and/or tailing, which would normally indicate species interconversion. In order to investigate this further, IMS^2 experiments were performed in which each of the features observed were isolated and activated. The presence of the same ATD with only a single peak for each of the non-activated and activated features indicated this was not the case (Figure S-3), with the additional species observed at higher number of cycles likely being due to components that were unresolved at a lower number of cycles.

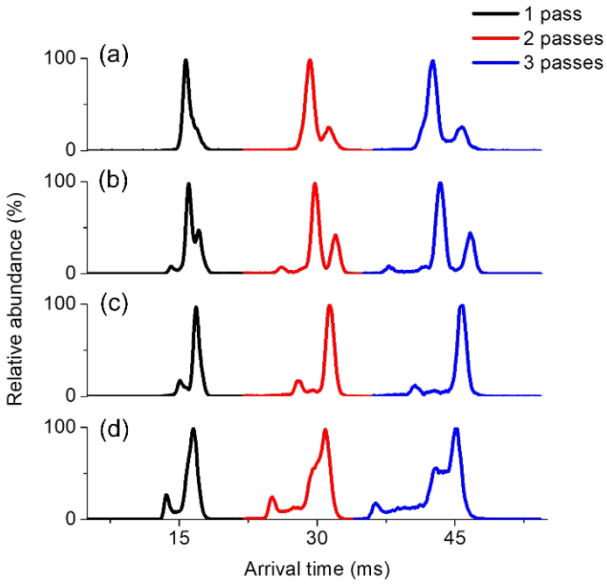

Figure 3. Arrival time distributions (ATDs) of doubly-derivatized monosaccharides (m/z 529.04) including (a) fructose, (b) galactose, (c) glucose, and (d) mannose with a varying number of passes using the cIM instrument. Sections of the ATDs without features were truncated for clarity.

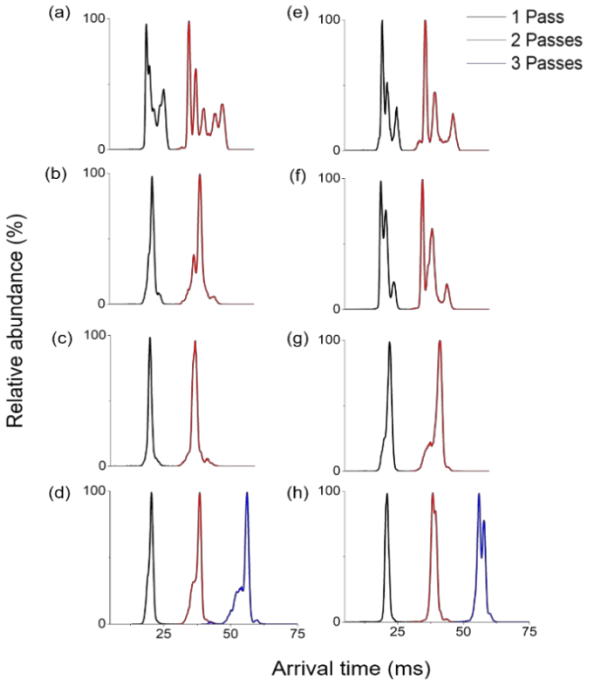

Figure 4. Doubly-derivatized disaccharides analyzed on the cyclic IM instrument. The studied disaccharides were (a) cellobiose, (b) isomaltose, (c) lactose, (d) lactulose, (e) maltose, (f) melibiose, (g) sucrose, and (h) trehalose. Only two passes are shown in cases where the wraparound effect was observed after three passes.

It is of interest to compare the separation of the most abundant species of each of the pairs of mono- and disaccharides after three

passes around cIM with that obtained using the SYNAPT instrument incorporating the linear TWIMS device. Figures S-4 and S-5 show ATDs of doubly derivatized monosaccharides and disaccharides obtained on the two platforms. The two-peak resolution ($R_{pp} = 1.18 \frac{t_{dB} - t_{dA}}{\Delta t_{dB} + \Delta t_{dA}}$)[34] was calculated for all possible pairs of monosaccharides and disaccharides to enable quantitative comparisons (Tables S-2 and S-3). The R_{pp} values calculated from cIM data were (expectedly) higher than the corresponding SYNAPT values, with one notable exception. For isomaltose *vs.* melibiose, the R_{pp} was the same for both platforms. We attributed this observation to the presence of several closely related structures. This phenomenon has been well documented for protein ions, with examples including Koeniger *et al.,*[48] Allen *et al.,* [49] and Eldrid *et al*.[39] For both melibiose and isomaltose, we predicted 5 possible derivatives, but only three asymmetric features were observed in the ATDs, suggesting the presence of more, unresolved components.

Tandem mass spectrometry

The ATD features that are resolved after 3 passes were investigated in more detail using post-IM collision induced dissociation (CID). Because no further IM separation takes place, ATDs of product ions are time-aligned with precursor ATD features. Thus, diagnostic product ions can be used to deduce 3C5NBA derivatization sites in precursor isomers as well as to identify isomers not fully resolved in ATD space.

The proposed structural assignments of features resolved in the ATD of doubly-derivatized maltose provide an interesting example of the post-IM CID capabilities of the cIM system (Figure 5). Four main mobility features were identified (I-IV), with corresponding CID product ion spectra presented in Figure S-6 a-d, respectively. The ATD for each of these fragments is shown in Figure S-7. Certain fragments aligned almost entirely with a single ATD peak, such as *m/z* 654, 485, and 451 aligned with feature I, II, and IV, respectively (Figure S-7a,d,e). Most fragments aligned with at least two of the peaks, such as *m/z* 529 and 354 (Figure 7-b,i). A summary of the correlation of each fragment's *m/z* and arrival time distribution is shown in Figure S-8. The dominant *m/z* peaks produced from feature I were *m/z* 396 ($C_{15}H_{15}BNO_{11}$), 294 ($C_{11}H_9BNO_8$), and 354 ($C_{13}H_{13}BNO_{10}$), which corresponded to a 3,4 cross-ring cleavage on the former reducing end of the sugar, a 1,2 cross-ring cleavage on the non-reducing end, and a cleavage of the glycosidic bond followed by a proton transfer, respectively (Figure 5). These fragments are only plausible for a derivative with each 3C5NBA molecule on a separate glucose residue, such as the product shown in Figure 2d. The most abundant product ions that originated from feature II are *m/z* 485 ($C_{19}H_{15}B_2N_2O_{12}$), which was produced by a 2,6 ring cleavage followed by a proton transfer, 353 ($C_{13}H_{12}BNO_{10}$) from a loss of one 3-carboxy-5-nitrophenyl-borane (** in Figure 5) and a cleavage of the glycosidic bond, 396 ($C_{15}H_{15}BNO_{11}$), from the same ** loss followed by a 3,4 ring cleavage on the former reducing end of the sugar, and 294 ($C_{11}H_9BNO_8$), from the loss of ** followed by a 3,6 ring cleavage on the non-reducing end (Figure 5). For feature III, the major fragments were *m/z* 504 ($C_{18}H_{16}B_2N_2O_{14}$), which originated from a loss of ** followed by the cleavage of the glycosidic bond and 436 ($C_{18}H_{11}B_2N_2O_{10}$), originating from the cleavage of the glycosidic bond, a 1,4 ring cleavage, a loss of an oxygen atom, and a water loss (Figure 5). The most abundant fragments for feature IV are *m/z* 354 and 529, which have been described for other features as well as *m/z* 255 ($C_{12}H_7BNO_5$), which requires rearrangement to be produced. Interestingly, the diagnostic product ion at m/z 529 can only be produced by the 3C5NBA anhydride dimer reacting with two trans diols on the maltose unit (Figure 2a-c) and not with two 3C5NBA molecules reacting with two cis diols each on maltose. Certain fragments only appeared in significant yields for one feature, leading to the possibility for tentative structural identification, as shown in Figures 5 and S-5. For example, *m/z* 654 ($C_{26}H_{22}B_2N_2O_{17}$) was unique for feature I, m/z 485 ($C_{18}H_{19}BNO_{14}$) was unique for feature II, *m/z* 436 ($C_{17}H_8B_2N_2O_{11}$) was unique for feature III, and *m/z* 451 ($C_{18}H_{11}B_2N_2O_{11}$) was unique for feature IV.

IM-CID-MS experiments can also aid with identification of the carbohydrates investigated, which would be particularly beneficial for analysis of a mixture containing various saccharides. For example, based on 3-pass ATD information alone, mannose could not be mobility separated from glucose (R_{pp}=0.38); and fructose could not be separated from galactose (R_{pp}=0.53). However, the combined technique of IM-CID-MS distinguished mannose and glucose by their unique diagnostic product ions at *m/z* 438.97 for mannose and 402.96, 353.97, and 441.02 for glucose (Table S-4). Fructose and galactose also had unique product ions that distinguished them, as the fructose derivative produced the product ions at *m/z* 438.97 and 441.02, which galactose did not. Galactose produced product ions at *m/z* 353.97, 384.94, and 402.96, which fructose did not. Only galactose displayed a unique product ion at *m/z* 468.99.

For the eight disaccharide derivatives, unique product ions were seen for lactulose (*m/z* 493.08, 469.07), maltose (*m/z* 678.19, 558.10), melibiose (*m/z* 480.04), sucrose (*m/z* 194.89), and trehalose (*m/z* 675.15, 424.95), as described in Table S-5. Doubly-derivatized disaccharides that could not be differentiated based on IM separation alone were cellobiose/sucrose and isomaltose/lactulose/trehalose. Cellobiose generated diagnostic product ions at *m/z* 631.1, 485.023, and 456.03 that were not observed for sucrose (Table S-5). Isomaltose produced ions at *m/z* 631.10, 441.02, 409.03, 395.99, 349.00, and 275.92 that did not appear for either lactulose or trehalose (Table S-5). In summary, combining high-resolution IM separations with post IM CID is clearly useful for identifying these sugar derivatives and pursuing in depth analysis of their structural characteristics.

Analyst

ARTICLE

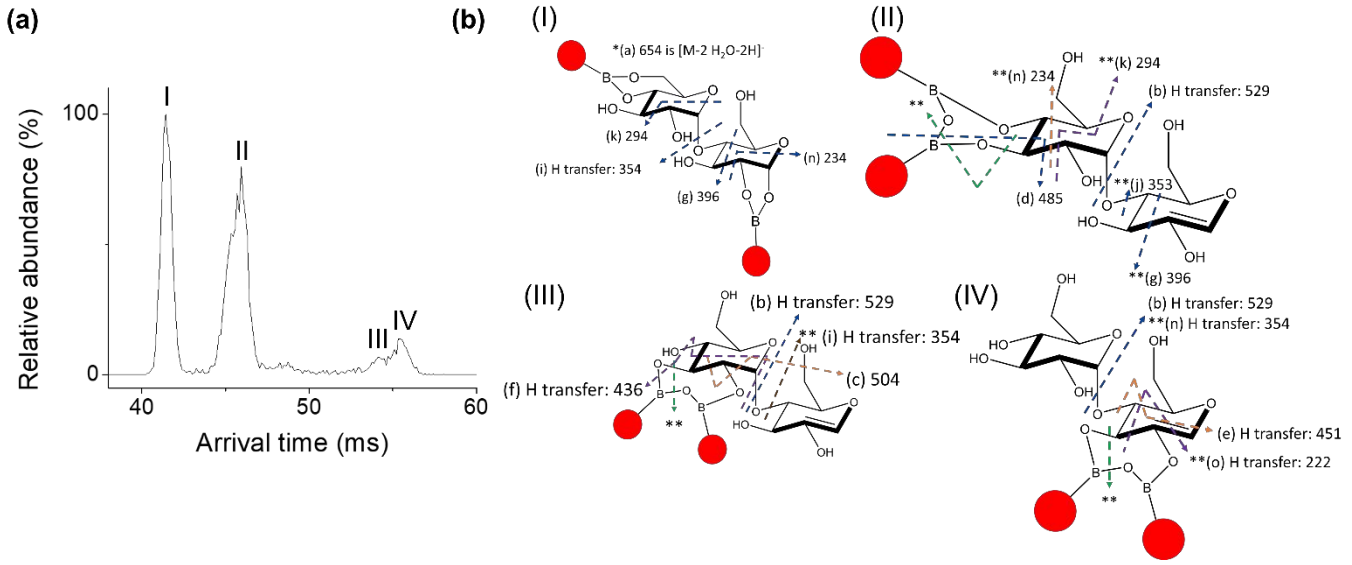

Figure 5. Post-IM CID experiment on doubly-derivatized maltose. (a) ATD of precursor ions after 3 passes around the cIM device; three features are resolved (I at 41.5 ms, II at 45.7 ms, and another feature formed from two partially unresolved peaks III at 52.8 ms and IV at 55.4 ms). (b) The proposed structural assignments for features I-IV in Figure 5 are based upon the fragmentation patterns shown. Fragment *m/z* correspond with Figure S-6: (a) 654 ($C_{26}H_{22}B_2N_2O_{17}$), (b) 529 ($C_{20}H_{17}B_2N_2O_{14}$), (c) 504 ($C_{18}H_{16}B_2N_2O_{14}$), (d) 485 ($C_{18}H_{19}BNO_{14}$), (e) 451 ($C_{18}H_{11}B_2N_2O_{11}$), (f) 436 ($C_{17}H_8B_2N_2O_{11}$), (g) 396 ($C_{15}H_{16}BNO_{11}$), (h) 392 ($C_{16}H_{16}BNO_{10}$), (i) 354($C_{13}H_{14}BNO_{10}$), (j) 353 ($C_{13}H_{13}BNO_{10}$), (k) 294 ($C_{11}H_{10}BNO_8$), (l) 281 ($C_{14}H_9BNO_5$), (m) 255 ($C_{12}H_7BNO_5$), (n) 234 ($C_9H_6BNO_6$), and (o) 222 ($C_8H_6BNO_6$). Fragments h, l, and m require rearrangements and are therefore not included in this Figure. ** represents a loss of one 3-carboxy-5-nitrophenyl-borane group.

Conclusions

Separations with cIM allowed for the identification and structural characterisation of 3C5NBA derivatives of mono- and disaccharides. After 3 passes around the cIM device (R_p~120), 3C5NBA carbohydrate derivatives were resolved in all cases for four monosaccharide standards, and all but two cases for eight disaccharide standards. Additional passes could improve separations of isomers with overlapping ATDs; however, there is a limit to the number of additional passes that maybe performed. In the future, novel cIM methods using a selection based upon ion mobility in an analogous way to heartcuts in chromatography will help to overcome these issues.[36-37] This would allow for a greater number of passes to be performed for these analytes, which would further enhance separations. With the improved resolving power made accessible by these techniques, cIM-MS/MS may be a viable method to characterize complex mixtures of carbohydrates. These methods could then be utilized to study mixtures of carbohydrates formed under abiotic conditions, which are currently under investigation in our laboratory.

Conflicts of interest

There are no conflicts to declare.

Acknowledgements

This work was jointly supported by NSF and the NASA Astrobiology Program, under the NSF Center for Chemical Evolution, CHE-1504217.

References

(1) Lazcano, A.; Miller, S. L., *Cell* **1996,** *85* (6), 793-798.
(2) Miller, S. L., *Science* **1953,** *117* (3046), 528-529.
(3) Fox, S. W.; Harada, K., *Science* **1958,** *128* (3333), 1214.
(4) Oró, J., *Nature* **1961,** *191*, 1193-1194.
(5) Weber, A. L., *J. Mol. Evol.* **1992,** *35* (1), 1-6.
(6) Gamblin, D. P.; Scanlan, E. M.; Davis, B. G., *Chem. Rev.* **2009,** *109* (1), 131-163.
(7) Krogh, A.; Lindhard, J., *Biochem. J* **1920,** *14* (3-4), 290-363.
(8) Abbott, D. W.; Ficko-Blean, E.; van Bueren, A. L.; Rogowski, A.; Cartmell, A.; Coutinho, P. M.; Henrissat, B.; Gilbert, H. J.; Boraston, A. B., *Biochemistry* **2009,** *48* (43), 10395-10404.
(9) de la Fuente, J. M.; Penadés, S., *Glycoconjugate J.* **2004,** *21* (3), 149-163.
(10) Dennis, J. W.; Granovsky, M.; Warren, C. E., *Bioessays* **1999,** *21* (5), 412-21.
(11) Tolstoguzov, V., *Carbohydr. Polym.* **2003,** *54* (3), 371-380.
(12) Fry, S. C., *Planta* **1983,** *157* (2), 111-123.
(13) Dell, A.; Morris, H. R.; Easton, R. L.; Panico, M.; Patankar, M.;

Oehninger, S.; Koistinen, R.; Koistinen, H.; Seppala, M.; Clark, G. F., *J. Biol. Chem.* **1995,** *270* (41), 24116-24126.
(14) Mottram, D. S.; Wedzicha, B. L.; Dodson, A. T., *Nature* **2002,** *419* (6906), 448-449.
(15) Schramm, G.; Grötsch, H.; Pollmann, W., *Angewandte Chemie International Edition in English* **1962,** *1* (1), 1-7.
(16) Stern, R.; Jedrzejas, M. J., *Chem. Rev.* **2008,** *108* (12), 5061-85.
(17) Azenha, C. S.; Coimbra, M. A.; Moreira, A. S.; Domingues, P.; Domingues, M. R., *J. Mass Spectrom.* **2013,** *48* (5), 548-52.
(18) Kuki, Á.; Szabó, K. E.; Nagy, L.; Zsuga, M.; Kéki, S., *J. Mass Spectrom.* **2013,** *48* (12), 1276-1280.
(19) Xing, X.; Hsieh, Y. S. Y.; Yap, K.; Ang, M. E.; Lahnstein, J.; Tucker, M. R.; Burton, R. A.; Bulone, V., *Carbohydr. Polym.* **2017,** *175* (Supplement C), 231-240.
(20) Agrawal, P. K., *Phytochemistry* **1992,** *31* (10), 3307-3330.
(21) Armstrong, G. S.; Mandelshtam, V. A.; Shaka, A. J.; Bendiak, B., *J. Magn. Reson.* **2005,** *173* (1), 160-168.
(22) Koizumi, K.; Okada, Y.; Fukuda, M., *Carbohydr. Res.* **1991,** *215* (1), 67-80.
(23) Zhou, S.; Huang, Y.; Dong, X.; Peng, W.; Veillon, L.; Kitagawa, D. A. S.; Aquino, A. J. A.; Mechref, Y., *Anal. Chem.* **2017,** *89* (12), 6590-6597.
(24) Stadlmann, J.; Weber, A.; Pabst, M.; Anderle, H.; Kunert, R.; J. Ehrlich, H.; Peter Schwarz, H.; Altmann, F., *Proteomics* **2009,** *9* (17), 4143-4153.
(25) Robinson, L. N.; Artpradit, C.; Raman, R.; Shriver, Z. H.; Ruchirawat, M.; Sasisekharan, R., *Electrophoresis* **2012,** *33* (5), 797-814.
(26) Mantovani, V.; Galeotti, F.; Maccari, F.; Volpi, N., *Electrophoresis* **2018,** *39* (1), 179-189.
(27) Siems, W. F.; Wu, C.; Tarver, E. E.; Hill, H. H., Jr.; Larsen, P. R.; McMinn, D. G., *Anal. Chem.* **1994,** *66* (23), 4195-4201.
(28) Clemmer, D. E.; Jarrold, M. F., *J. Mass Spectrom.* **1997,** *32* (6), 577-592.
(29) Giles, K.; Pringle, S. D.; Worthington, K. R.; Little, D.; Wildgoose, J. L.; Bateman, R. H., *Rapid Commun. Mass Spectrom.* **2004,** *18* (20), 2401-2414.
(30) Ruotolo, B. T.; Benesch, J. L. P.; Sandercock, A. M.; Hyung, S. J.; Robinson, C. V., *Nature Protocols* **2008,** *3* (7), 1139-1152.
(31) Smith, D. P.; Knapman, T. W.; Campuzano, I.; Malham, R. W.; Berryman, J. T.; Radford, S. E.; Ashcroft, A. E., *Eur. J. Mass Spectrom.* **2009,** *15* (2), 113-130.
(32) Thalassinos, K.; Grabenauer, M.; Slade, S. E.; Hilton, G. R.; Bowers, M. T.; Scrivens, J. H., *Anal. Chem.* **2009,** *81* (1), 248-254.
(33) Bush, M. F.; Hall, Z.; Giles, K.; Hoyes, J.; Robinson, C. V.; Ruotolo, B. T., *Anal. Chem.* **2010,** *82* (22), 9557-9565.
(34) Dodds, J. N.; May, J. C.; McLean, J. A., *Anal. Chem.* **2017,** *89* (22), 12176-12184.
(35) Kevin Giles, J. U., Jason Wildgoose, Martin R. Green, Keith Richardson, David Langridge, Nick Tomczyk In *Design and performance of a second-generation cyclic ion mobility enabled Q-ToF*, 65th ASMS Conference, Indianapolis, IN, Indianapolis, IN, 2017.
(36) Giles, K.; Ujma, J.; Wildgoose, J.; Pringle, S.; Richardson, K.; Langridge, D.; Green, M., *Anal. Chem.* **2019**.
(37) Ujma, J.; Ropartz, D.; Giles, K.; Richardson, K.; Langridge, D.; Wildgoose, J.; Green, M.; Pringle, S., *J. Am. Soc. Mass. Spectrom.* **2019,** *30* (6), 1028-1037.
(38) Ropartz, D.; Fanuel, M.; Ujma, J.; Palmer, M.; Giles, K.; Rogniaux, H., *Anal. Chem.* **2019,** *91* (18), 12030-12037.
(39) Eldrid, C.; Ujma, J.; Kalfas, S.; Tomczyk, N.; Giles, K.; Morris, M.; Thalassinos, K., *Anal. Chem.* **2019,** *91* (12), 7554-7561.
(40) Huang, Y.; Dodds, E. D., *Anal. Chem.* **2013,** *85* (20), 9728-9735.
(41) Huang, Y.; Dodds, E. D., *Anal. Chem.* **2015,** *87* (11), 5664-5668.
(42) Yang, H.; Shi, L.; Zhuang, X.; Su, R.; Wan, D.; Song, F.; Li, J.; Liu, S., *Sci. Rep.* **2016,** *6*.
(43) Li, L.; McKenna, K. R.; Li, Z.; Yadav, M.; Krishnamurthy, R.; Liotta, C. L.; Fernandez, F. M., *Analyst* **2018,** *143* (4), 949-955.
(44) Forsythe, J. G.; Petrov, A. S.; Walker, C. A.; Allen, S. J.; Pellissier, J. S.; Bush, M. F.; Hud, N. V.; Fernandez, F. M., *Analyst* **2015,** *140* (20), 6853-61.
(45) Giles, K.; Wildgoose, J. L.; Pringle, S.; Langridge, D. J.; Nixon, P.; Garside, J.; Carney, P., *Characterising A T-Wave Enabled Multi-pass Cyclic Ion Mobility Separator* **2015**.
(46) Hess, D.; Klufers, P., *Carbohydr. Res.* **2011,** *346* (13), 1752-9.
(47) Meiland, M.; Heinze, T.; Guenther, W.; Liebert, T., *Tetrahedron Lett.* **2009,** *50* (4), 469-472.
(48) Koeniger, S. L.; Clemmer, D. E., *J. Am. Soc. Mass. Spectrom.* **2007,** *18* (2), 322-331.
(49) Allen, S. J.; Giles, K.; Gilbert, T.; Bush, M. F., *Analyst* **2016,** *141* (3), 884-891.

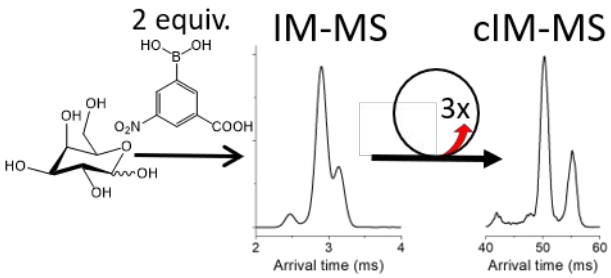

Cyclic ion mobility-tandem mass spectrometry enhances the separation and identification of small carbohydrate isomers.